Composition Space of the (CuO, $^1/_2Nb_2O_5$)/$(HF)_x$·pyridine/H_2O System. Structure and Synthesis of $[pyH^+]_2[CuNb_2(py)_4O_2F_{10}]^{2-}$ and $CuNb(py)_4OF_5$

Paramasivan Halasyamani,[†] Michael J. Willis,[†] Charlotte L. Stern,[†] Paul M. Lundquist,[§] George K. Wong,[§] and Kenneth R. Poeppelmeier*,[‡]

Materials Research Center and Departments of Chemistry and Physics and Astronomy, Northwestern University, Evanston, Illinois 60208

Received September 11, 1995[⊗]

Single crystals of $[pyH^+]_2[CuNb_2(py)_4O_2F_{10}]^{2-}$ and $CuNb(py)_4OF_5$ were synthesized in a $(HF)_x$·pyridine/pyridine/water solution (150 °C, 24 h, autogeneous pressure) using CuO and Nb_2O_5 as reagents. The compound $[pyH^+]_2[CuNb_2(py)_4O_2F_{10}]^{2-}$ contains clusters of $[CuNb_2(py)_4O_2F_{10}]^{2-}$ anions linked through $N-H^+\cdots F$ hydrogen bonds to the $[pyH^+]$ cations. In contrast $CuNb(py)_4OF_5$ is a unidimensional compound consisting only of chains, perpendicular to the *c* axis, of alternating $[Cu(py)_4(O/F)_{2/2}]^{0.5+}$ and $[NbF_4(O/F)_{2/2}]^{0.5-}$ octahedra. The chains change direction between the [*110*] and [$1\bar{1}0$] every *c*/2. Crystal data for $[pyH^+]_2[CuNb_2(py)_4O_2F_{10}]^{2-}$: tetragonal, space group $I4_122$ (No. 98),with $a = 11.408(3)$ Å, $c = 30.36(1)$ Å, and $Z = 4$. Crystal data for $CuNb(py)_4OF_5$: monoclinic, space group $C2/c$ (No. 15), with $a = 10.561(3)$ Å, $b = 13.546(6)$ Å, $c = 16.103(4)$ Å, $\beta = 97.77(2)°$, and $Z = 4$.

Introduction

Goodenough and Longo[1] and Kunz and Brown[2] have shown that d^0 transition metal oxides are unstable with respect to *intraoctahedral* distortions. Out-of-center distortions can be understood through the second-order Jahn−Teller theorem[3−5] and are postulated to be one cause of ferroelectric behavior.[6] The out-of-center distortion commonly observed in $[NbOF_5]^{2-}$ octahedra is structurally similar to the C_4 distortion observed in the $[NbO_{6/2}]^-$ octahedron (e.g $LiNbO_3$;[7] see Figure 1), which is postulated to be the origin of the large second-order NLO response in oxide ferroelectrics.[8,9]

One goal of this research is to gain insight into the structure−property relationships in well-known ferroelectrics and technologically important NLO oxides, such as $BaTiO_3$, $KTiOPO_4$, and $LiNbO_3$, in order to promote novel synthetic routes to new materials with interesting magnetic, electronic, and optical properties.[10−15] The combination of first- and second-order Jahn−Teller ions is one approach that can be used to design d^0 transition metal cations in a stable bonding network. Known first-order Jahn−Teller (FOJT) and second-order Jahn−Teller (SOJT) mixed-metal Cu^{II}/Nb^V oxyfluorides, which combine d^9 Cu^{II} with d^0 Nb^V through corner- or edge-shared octahedra, are $Cu_{0.6}Nb_6O_{14.6}F_{1.4}$,[16] $CuNbO_3F$,[17] and $CuNb(OH,F)_7·3H_2O$.[18] In this paper the structures, syntheses, infrared spectra, and magnetic susceptibilities of two new copper niobium oxyfluorides, $[pyH^+]_2[CuNb_2(py)_4O_2F_{10}]^{2-}$ and $CuNb(py)_4OF_5$, are reported. Conditions for selective crystallization, from the (CuO, $^1/_2Nb_2O_5$)/$(HF)_x$·pyridine/H_2O system in excess pyridine, are presented.

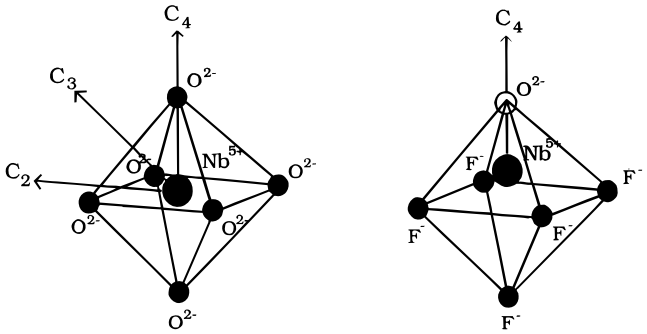

Figure 1. Intraoctahedral distortions in $[NbO_{6/2}]^-$ (e.g. $LiNbO_3$) and $[NbOF_5]^{2-}$ octahedra.

Experimental Section

Caution. $(HF)_x$·pyridine is toxic and corrosive!

Materials. CuO (99.99%, Aldrich), Nb_2O_5 (99.99%, Aldrich), pyridine (99.9%, anhydrous, Aldrich), and $(HF)_x$·pyridine (pyridinium poly(hydrogen fluoride), 70% HF by weight, Aldrich) were used as received. Reagent amounts of deionized H_2O were also used in the synthesis.

Synthesis. The compound $[pyH^+]_2[CuNb_2(py)_4O_2F_{10}]^{2-}$ was synthesized by adding 3.98×10^{-2} g (5×10^{-4} mol) of CuO and 6.65 ×

* To whom correspondence should be addressed.
[†] Department of Chemistry.
[‡] Materials Research Center and Department of Chemistry.
[§] Materials Research Center and Department of Physics and Astronomy.
[⊗] Abstract published in *Advance ACS Abstracts,* February 1, 1996.

(1) Goodenough, J. B.; Longo, J. M. Crystallographic and magnetic properties of perovskite and perovskite-related compounds. In *Landolt-Bornstein*; Hellwege, K. H., Hellwege, A. M., Eds.; Springer-Verlag: Berlin, 1970; Vol. 4, pp 126−314.
(2) Kunz, M.; Brown, I. D. *J. Solid State Chem.* **1995**, *115*, 395.
(3) Wheeler, R. A.; Whangbo, M. H.; Hughbanks, T.; Hoffman, R.; Burdett, J. K.; Albright, T. A. *J. Am. Chem. Soc.* **1986**, *108*, 2222.
(4) Kang, S. K.; Tang, H.; Albright, T. A. *J. Am. Chem. Soc.* **1993**, *115*, 1971.
(5) Cohen, R. E. *Nature* **1992**, *358*, 136.
(6) Munowitz, M.; Jarman, R. H.; Harrison, J. F. *Chem. Mater.* **1993**, *5*, 661.
(7) Matthias, B. T.; Remeika, J. P. *Phys. Rev.* **1949**, *76*, 1886.
(8) DiDomenico, M.; Wemple, S. H. *J. Appl. Phys.* **1969**, *20*, 720.
(9) Chen, C.; Liu, G. *Annu. Rev. Mater. Sci* **1986**, *16*, 203.
(10) Kay, H. F.; Wellard, H. J.; Vousden, P. *Nature* **1949**, *163*, 636.
(11) Abrahams, S. C.; Reddy, J. M.; Bernstein, J. L. *J. Phys. Chem. Solids* **1966**, *27*, 997.
(12) Phillips, M. L.; Gier, T. E.; Eddy, M. M.; Keder, N. L.; Stucky, G. D.; Bierlein, J. D. *Solid State Ionics* **1989**, *32/33*, 147.
(13) Stucky, G. D.; Phillips, M. L. F.; Gier, T. E. *Chem. Mater.* **1989**, *1*, 492.
(14) Phillips, M. L. F.; Harrison, W. T. A.; Gier, T. E.; Stucky, G. D.; Kulkarni, G. V.; Burdett, J. K. *Inorg. Chem.* **1990**, *29*, 2158.
(15) Hagerman, M. E.; Poeppelmeier, K. R. *Chem. Mater.* **1995**, *7*, 602.
(16) Wallunga, P. N. *Acta Chem. Scand.* **1984**, *38A*, 641.
(17) Lundberg, M.; Savborg, O. *Chem. Scr.* **1978**−79, *13*, 197.
(18) Lopez-Crosnier, M. P.; Duroy, H.; Fourquet, J. L. *J. Solid State Chem.* **1994**, *108*, 398.

0020-1669/96/1335-1367$12.00/0

Table 1. Crystallographic Data for $[pyH^+]_2[CuNb_2(py)_4O_2F_{10}]^{2-}$ and $CuNb(py)_4OF_5$

formula $C_{30}H_{32}CuF_{10}N_6Nb_2O_2$	$T = -120(1)$ °C
fw 947.96	$\lambda = 0.710\ 69$ Å
space group $I4_122$ (No. 98)	$\rho_{calcd} = 1.593$ g/cm^3
$a = 11.408(3)$ Å	$\rho_{obsd} = 1.58(1)^a$ g/cm^3
$c = 30.36(1)$ Å	$\mu = 11.85$ cm^{-1}
$V = 3951(2)$ Å^3	$R(F)^b = 0.043$
$Z = 4$	$R_w(F)^c = 0.044$
formula $C_{20}H_{20}CuF_5N_4NbO$	$T = -100(1)$ °C
fw 583.85	$\lambda = 0.710\ 69$ Å
space group $C2/c$ (No. 15)	$\rho_{calcd} = 1.699$ g/cm^3
$a = 10.561(3)$ Å	$\rho_{obsd} = 1.69(1)^a$ g/cm^3
$b = 13.546(6)$ Å	$\mu = 14.72$ cm^{-1}
$c = 16.103(4)$ Å	$R(F)^b = 0.026$
$\beta = 97.77(2)°$	$R_w(F)^c = 0.038$
$V = 2282(2)$ Å^3	
$Z = 4$	

[a] Density measured by flotation pycnometry at 24 °C. [b] $R = \sum||F_o| - |F_c||/\sum|F_o|$. [c] $R_w = [\sum w(|F_o| - |F_c|)^2/\sum w(F_o)^2]^{1/2}$.

10^{-2} g (2.5×10^{-4} mol) Nb_2O_5 to a Teflon "pouch".[19] To this mixture were added 8.6×10^{-1} g (2.5×10^{-3} mol) of $(HF)_x$·pyridine, 3.6×10^{-2} g (2.0×10^{-3} mol) of H_2O, and 7.9×10^{-1} g (1×10^{-2} mol) of pyridine. $CuNb(py)_4OF_5$ was synthesized by adding 3.98×10^{-2} g (5×10^{-4} mol) of CuO and 6.65×10^{-2} g (2.5×10^{-4} mol) of Nb_2O_5 to a separate Teflon "pouch". To this mixture were added 5.1×10^{-1} g (1.5×10^{-3} mol) of $(HF)_x$·pyridine, 9.0×10^{-2} g (5×10^{-3} mol) of H_2O, and 7.9×10^{-1} g (1×10^{-2} mol) of pyridine.

IR ($CuNb(py)_4OF_5$, KBr): ν(Nb−O) = 890 cm^{-1}, ν(Nb−F) = 590 cm^{-1}, ν(Nb−F) = 550 cm^{-1}.

IR ($[pyH^+]_2[CuNb_2(py)_4O_2F_{10}]^{2-}$, KBr): ν(Nb−O) = 900 cm^{-1}, ν(Nb−F) = 585 cm^{-1}, ν(Nb−F) = 530 cm^{-1}, ν(pyH$^+$) = 1630, 1531, 1337, and 1259 cm^{-1}.

The pouches were sealed and placed in a 2000 mL autoclave (Parr) filled with 600 mL of water. The autoclave was heated for 24 h at 150 °C and cooled to room temperature over an additional 24 h. The pouches were removed from the autoclave and opened in air, and the products, large deep blue crystals, were recovered by filtration. The products, subsequently determined to be $[pyH^+]_2[CuNb_2(py)_4O_2F_{10}]^{2-}$ and $CuNb(py)_4OF_5$, were recovered in about 40% and 60% yields, respectively, based on copper oxide.

Crystallographic Determination. Crystallographic data, atomic coordinates and isotropic thermal parameters, and selected bond distances and angles for $[pyH^+]_2[CuNb_2(py)_4O_2F_{10}]^{2-}$ and $CuNb(py)_4OF_5$ are given in Tables 1−3, respectively. For both compounds crystal quality was determined by Weissenberg photography. All calculations were done using the TEXSAN[20] crystallographic software package from Molecular Structure Corp. The structures were solved by Patterson map (SHELXS-86)[21] and expanded using Fourier techniques.[22]

Crystal Structure of $[pyH^+]_2[CuNb_2(py)_4O_2F_{10}]^{2-}$. On the basis of systematic absences and successful solution and refinement of the structure, the space group was determined to be $I4_122$ (No. 98). During the refinement it was determined that the asymmetric unit contains only three unique atoms for the pyridinium molecule, indicating disorder between nitrogen and carbon. Because a variety of disorder configurations are possible, potential hydrogen-bonding interactions were used to constrain N(3) and C(9) over the same general position, resulting in N(3)−H$^+$···F(3) interactions. All non-hydrogen atoms except for N(3) and C(9) were refined anisotropically, with the hydrogen atoms placed in idealized positions. The atomic coordinates were inverted, and the structure was re-refined. The reported coordinates are those resulting in the lower $R(F)$ value.

Crystal Structure of $CuNb(py)_4OF_5$. Four octants of data, hkl, $\bar{h}k\bar{l}$, $hk\bar{l}$, and $\bar{h}\bar{k}l$, were collected (instead of the minimum two required for a monoclinic cell) to compare Friedel pairs. Data averaging was only performed after it was determined that the acentric refinement (Cc (No. 9)) was ill-behaved. On the basis of systematic absences

Table 2. Atomic Coordinates of $[pyH^+]_2[CuNb_2(py)_4O_2F_{10}]^{2-}$ and $CuNb(py)_4OF_5$

atom	site	x	y	z	B_{eq}[a], Å^2
		$[pyH^+]_2[CuNb_2(py)_4O_2F_{10}]^{2-}$			
Nb	8e	0.75696(7)	0.7600	0.5000	1.59(2)
Cu	4a	0.5000	0.5000	0.5000	0.89(5)
F(1)	16g	0.8868(4)	0.6507(5)	0.4911(2)	1.9(3)
F(2)	16g	0.7859(4)	0.7532(4)	0.5626(1)	1.8(2)
F(3)	8e	0.8871(4)	0.8871	0.5000	3.9(4)
O(1)	8e	0.6493(5)	0.6493	0.5000	1.0(2)
N(1)	8c	0.5000	0.5000	0.5676(3)	1.4(7)
N(2)	8d	0.3722(6)	0.6280	0.5000	1.5(3)
N(3)	16g	0.955(1)	0.961(1)	0.4141(3)	2.5(3)[b]
C(1)	16g	0.573(2)	0.564(2)	0.5904(3)	5.2(4)
C(2)	16g	0.579(2)	0.563(2)	0.6354(3)	4.7(4)
C(3)	8c	0.5000	0.5000	0.6591(3)	2.5(5)
C(4)	16g	0.2624(9)	0.6031(7)	0.4906(5)	3.2(3)
C(5)	16g	0.174(1)	0.685(1)	0.4916(5)	4.0(3)
C(6)	8d	0.1997(8)	0.8000	0.5000	2.9(2)
C(7)	16g	0.917(2)	0.916(2)	0.3758(4)	5(1)
C(8)	16g	0.962(2)	0.954(2)	0.3369(4)	6.4(4)
C(9)	16g	0.957	0.959	0.4140	2.5[b]
		$CuNb(py)_4OF_5$			
Nb	4b	0.0000	0.5000	0.000	2.038(6)
Cu	4d	0.2500	0.7500	0.000	1.700(6)
F(1)	8f	−0.0445(1)	0.5417	−0.10752(7)	3.02(3)
F(2)	8f	0.1350(1)	0.4190(1)	0.05540(8)	3.27(3)
F(3)	8f	0.1181	0.6094	0.0025	2.00[b]
O(1)	8f	0.1181(1)	0.6094(1)	0.0025(1)	2.00(2)[b]
N(1)	8f	0.0925(2)	0.8353(1)	−0.0347(1)	1.97(3)
N(2)	8f	0.2625(2)	0.7289(1)	−0.12658(9)	1.95(3)
C(1)	8f	−0.0226(2)	0.8076(2)	−0.0156(1)	2.44(3)
C(2)	8f	−0.1334(2)	0.8590(2)	−0.0428(2)	3.18(4)
C(3)	8f	−0.1263(2)	0.9424(2)	0.0930(1)	3.40(4)
C(4)	8f	−0.0084(3)	0.9709(2)	−0.1132(1)	3.33(5)
C(5)	8f	0.0994(2)	0.9167(2)	−0.0817(1)	2.52(2)
C(6)	8f	0.1895(2)	0.6570(1)	−0.1673(1)	2.38(3)
C(7)	8f	0.1887(2)	0.6404(2)	−0.2529(1)	2.85(3)
C(8)	8f	0.2612(2)	0.6996(2)	−0.2973(1)	3.20(4)
C(9)	8f	0.3325(2)	0.7767(2)	−0.2562(1)	3.26(4)
C(10)	8f	0.3308(2)	0.7865(2)	−0.1698(1)	2.78(4)

[a] $B_{eq} = (8/3)\pi^2(U_{11}(aa^*)^2 + U_{22}(bb^*)^2 + U_{33}(cc^*)^2 + 2U_{12}aa^*bb^* \cos\gamma + 2U_{13}aa^*cc^* \cos\beta + 2U_{23}bb^*cc^* \cos\alpha)$. [b] Isotropic refinement. Site occupancy factors for these atoms are 0.5.

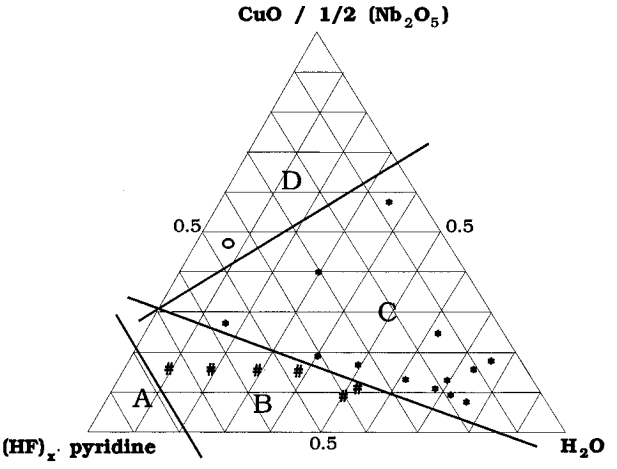

Figure 2. Composition space of (CuO, $^1/_2Nb_2O_5$)/$(HF)_x$·pyridine/H_2O in excess pyridine. The four synthetic regions (A−D) are shown (see text).

(19) Gier, T. E.; Stucky, G. D. *Nature* **1991**, *349*, 508.
(20) *TEXSAN-TEXRAY Structure Analysis Package*; Molecular Structure Corp.: The Woodlands, TX, 1985.
(21) Sheldrick, G. M. SHELXS86. In *Crystallographic Computing 3*. Sheldrick, G. M., Kruger, C., Goddard, R., Eds.; Oxford University Press: Oxford, U.K., 1985; pp 175−189.
(22) Beurskins, P. T.; Admiraal, G.; Beurskens, G.; Bosman, W. P.; Garcia-Granda, S.; Gould, R. O.; Smits, J. M. M.; Smykalla, C. DIRDIF92. The DIRDIF program system, Technical Report; Crystallography Laboratory, University of Nijmegen: Nijmegen, The Netherlands, 1992.

Table 3. Principal Bond Distances (Å) and Angles (deg) in $[pyH^+]_2[CuNb_2(py)_4O_2F_{10}]^{2-}$ and $CuNb(py)_4OF_5$

	$[pyH^+]_2[CuNb_2(py)_4O_2F_{10}]^{2-}$		
	Bond Distances		
Nb−F(1)	1.937(6)	Cu−N(1)	2.06(1)
Nb−F(2)	1.927(5)	Cu−N(2)	2.06(1)
Nb−F(3)	2.099(8)	Cu−O(1)	2.417(9)
Nb−O(1)	1.728(8)		
N(3)···F(3)	2.85(1)		
	Bond Angles		
F(1)−Nb−F(1)*	168.7(2)	F(2)−Nb−F(2)*	167.9(3)
F(1)−Nb−F(2)	89.5(1)	F(2)−Nb−F(3)	84.0(2)
F(1)−Nb−F(3)	84.3(1)	F(2)−Nb−O(1)	96.0(1)
F(1)−Nb−O(1)	95.7(2)	F(3)−Nb−O(1)	180.0
		N(1)−Cu−N(2)	90.0
	$CuNb(py)_4OF_5$		
	Bond Distances		
Nb−F(1)	1.939(1)	Cu−N(1)	2.040(2)
Nb−F(2)	1.921(1)	Cu−N(2)	2.080(2)
Nb−F(3),O(1)	1.9340(2)	Cu−F(3),O(1)	2.3630(2)
	Bond Angles		
F(1)−Nb−F(1)*	180.0	F(2)*−Nb−F(3)	90.46(4)
F(1)−Nb−F(2)	89.64(6)	F(2)−Nb−F(3)	89.54(4)
F(1)−Nb−F(2)*	90.36(6)	N(1)−Cu−N(2)	88.08(6)
F(1)−Nb−F(3)	89.51(4)		
F(1)*−Nb−F(3)	90.49(4)		

and successful solution and refinement, the space group was determined to be *C*2/*c* (No. 15).

Spectroscopic Measurements. Mid-IR (400−4000 cm^{-1}) spectra were collected using a Bomem MB-100 Fourier transform infrared spectrophotometer equipped with a DTGS detector operating at a resolution of 2 cm^{-1}.

Susceptibility. Magnetic susceptibility measurements were performed on a Quantum Design Corp. MPMS SQUID susceptometer between 5 and 300 K. The measurements were done with single-crystal samples encased in sealed gelatin capsules. A 1-kG field was used for all measurements.

Nonlinear Optical Measurements. Second harmonic generation (SHG) measurements were performed on sifted (35−250 μm) $CuNb(py)_4OF_5$ powder using a center of symmetry classification technique described earlier.[23,24] Experiments were performed with blue and violet output from a tunable optical parametric amplifier[25] such that the fundamental and second harmonic wavelengths fell within the measured optical transmission window of $CuNb(py)_4OF_5$. No SHG was observed for any of the particle sizes, indicating that the chemical structure of the individual particulates was centrosymmetric.

Results

The composition space diagram for the (CuO, $^1/_2Nb_2O_5$)/(HF)$_x$·pyridine/H_2O system is shown in Figure 2. Two distinct crystallization fields occur in this system. In region D incomplete oxide dissolution was observed, with a blue solution, polycrystalline $CuNb(py)_4OF_5$, and unreacted oxides in the pouch after reaction. Crystals were grown in regions B and C. In region B the crystallization of $[pyH^+]_2[CuNb_2(py)_4O_2F_{10}]^{2-}$ occurs, and in region C the single crystals of $CuNb(py)_4OF_5$ were observed. Finally, in region A only a clear blue liquid was observed in the reaction pouches, as all species remain in solution. Susceptibility measurements of $[pyH^+]_2[CuNb_2(py)_4O_2F_{10}]^{2-}$ and $CuNb(py)_4OF_5$ indicated that the compounds were paramagnets, with μ_{eff}(300 K) = 1.89 μ_B and μ_{eff}(300 K) = 1.82 μ_B, respectively, values which are in excellent agreement

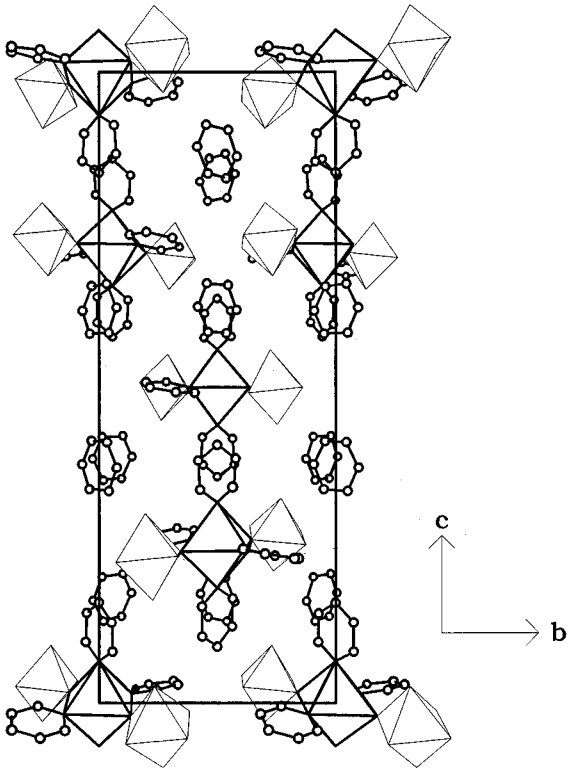

Figure 3. Packing diagram of $[pyH^+]_2[CuNb_2(py)_4O_2F_{10}]^{2-}$, with the light and dark outlined octahedra representing niobium and copper, respectively.

with those of other Cu^{II} complexes.[26,27] The data were corrected for core diamagnetism, using values from Mulay,[28] and the susceptibility of the gelatin capsule. A Curie−Weiss fit of the data resulted in, for $[pyH^+]_2[CuNb_2(py)_4O_2F_{10}]^{2-}$, $\chi_0 = -6.88 \times 10^{-4}$ emu/mol, $C_0 = 0.4468$ emu·K/mol, and $\Theta = -7.5 \times 10^{-3}$ K and, for $CuNb(py)_4OF_5$, $\chi_0 = -4.90 \times 10^{-5}$ emu/mol, $C_0 = 0.3616$ emu·K/mol, and $\Theta = -0.04102$ K. The negative values of the temperature-independent component of the susceptibility ($\chi_0 < 0$) indicate that Van Vleck diamagnetism dominates.[29]

Although both compounds are built up from linked units of $[Cu(py)_4]^{2+}$ and $[NbOF_5]^{2-}$, the manners in which these units combine are different. Given a constant mole fraction of oxides ((CuO, $^1/_2Nb_2O_5$) = 0.15; see Figure 2), the experimental results show that the synthesis of $[pyH^+]_2[CuNb_2(py)_4O_2F_{10}]^{2-}$ or $CuNb(py)_4OF_5$ is dependent on the (HF)$_x$·pyridine:H_2O ratio or, at an equimolar (HF)$_x$·pyridine:H_2O ratio, on the oxide concentration.

Bimetallic $[pyH^+]_2[CuNb_2(py)_4O_2F_{10}]^{2-}$ contains clusters of three corner-shared octahedra, with lattice pyridinium (pyH^+) cations in the open spaces between the clusters (see Figure 3). Cu^{II} is coordinated to four pyridines and two oxygens where the oxygens bridge to the $[NbOF_5]^{2-}$ octahedra. Nb^V is coordinated by five fluorines and one oxygen (see Figure 4). As seen in Figure 4, hydrogen bonding occurs through N(3)−H$^+$···F(3) interactions, linking the lattice pyridinium molecules to the cluster. Pyridinium was distinguished from the coordinated pyridine by infrared spectroscopy. The IR bands from coordinated pyridine are at 1611 and 637 cm^{-1}, shifted from

(23) Kurtz, S. K. *IEEE J. Quantum Electron.* **1968**, *QE4*, 578.
(24) Kurtz, S. K.; Perry, T. T. *J. Appl. Phys.* **1968**, *39*, 3798.
(25) Lundquist, P. M.; Yitzchaik, S.; Zhang, T.; Kanis, D. R.; Ratner, M. A.; Marks, T. J.; Wong, G. K. *Appl. Phys. Lett.* **1994**, *64*, 2194.
(26) Kido, K.; Watanabe, T. *J. Phys. Soc. Jpn.* **1959**, *14*, 1217.
(27) Figgis, B. N.; Gerloch, M.; Lewis, J.; Slade, R. C. *J. Chem. Soc. A* **1968**, 2028.
(28) Mulay, L. N. *Magnetic Susceptibility*; John Wiley and Sons: New York, 1963.
(29) Van Vleck, J. H. *Electric and Magnetic Susceptibilities*; Oxford University Press: London, 1932.

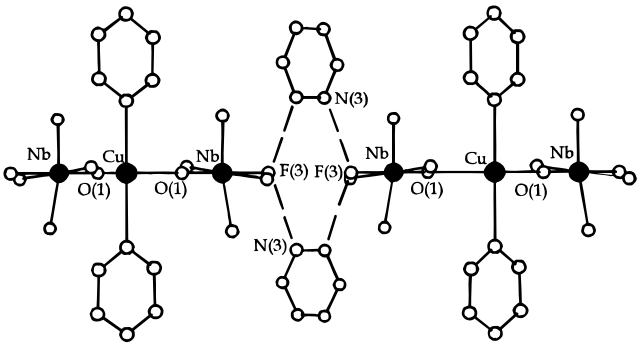

Figure 4. Ball-and-stick representation of $[pyH^+]_2[CuNb_2(py)_4O_2F_{10}]^{2-}$. Dashed lines indicate hydrogen bonding. An ORTEP (50% probability) plot is available in the Supporting Information.

those of the free base owing to coordination.[30] The pyridinium species had identifiable bands at 1630, 1531, 1337, and 1259 cm^{-1}, which agree with those previously reported.[30] $[pyH^+]_2[CuNb_2(py)_4O_2F_{10}]^{2-}$ has interesting structural features owing to the incorporation of acentric $[NbOF_5]^{2-}$ octahedra. The Nb^V cation in $[CuNb_2(py)_4O_2F_{10}]^{2-}$ is displaced toward the oxygen (d(Nb−F(3)) − d(Nb−O(1)) = 0.36(1) Å; see Table 3 and Figure 4), resulting in a strong intraoctahedral distortion collinear with the F(3)−Nb−O(1) bond.

The second compound discovered, $CuNb(py)_4OF_5$, was found to consist of continuous and nonintersecting chains of corner-shared copper and niobium octahedra. Each Cu^{II} is a d^9 Jahn−Teller-distorted cation with four short Cu−N equatorial bonds. The copper octahedron is completed by two longer axial bonds to fluorine and oxygen. The mean value of the four Cu−N bonds is 2.05(1) Å, while the Cu−O,F bond is 2.356(7) Å (Table 3 and Figure 5). The niobium octahedron is composed of four equatorial Nb−F bonds and two axial bonds, one to oxygen and the other to fluorine. The mean equatorial Nb−F bond distance is 1.92(2) Å, and the axial Nb−O,F bond length is 1.920(7) Å (Table 3 and Figure 5). The chains of octahedra alternate directions between the [*110*] and [$1\bar{1}0$] every *c*/2 (see Figure 6). The spaces between the chains are filled by pyridine molecules coordinated to the Cu^{II}. Owing to the preference of oxygen to be two-coordinate, it was inferred that the oxygen atoms bridge the metal centers and do not occupy equatorial sites. Infrared spectroscopy, with one Nb−O stretch at about 900 cm^{-1}, supports this assignment.

Discussion

The anhydrous nature of $(HF)_x$·pyridine permits the amount of added water to be carefully controlled and the construction of a composition space diagram (see Figure 2) which illustrates the products as a function of the mole fraction of each component. Well-defined crystallization regimes wherein selective crystal growth occurs have been determined. In region D, the excess amount of oxide relative to $(HF)_x$·pyridine results in a mixture of $CuNb(py)_4OF_5$ and unreacted reagent oxides. In regions B and C, the pyridinium poly(hydrogen fluoride) concentration appears to be a controlling factor in the crystal growth of $[pyH^+]_2[CuNb_2(py)_4O_2F_{10}]^{2-}$ versus $CuNb(py)_4OF_5$. The protonation of pyridine is decreased by both the addition of reagent H_2O (k_b(water) > k_b(pyridine)) and the dissolution of the oxides, which produces additional H_2O. Finally, owing to the high concentration of pyridinium poly(hydrogen fluoride) in region A, all species remain in solution.

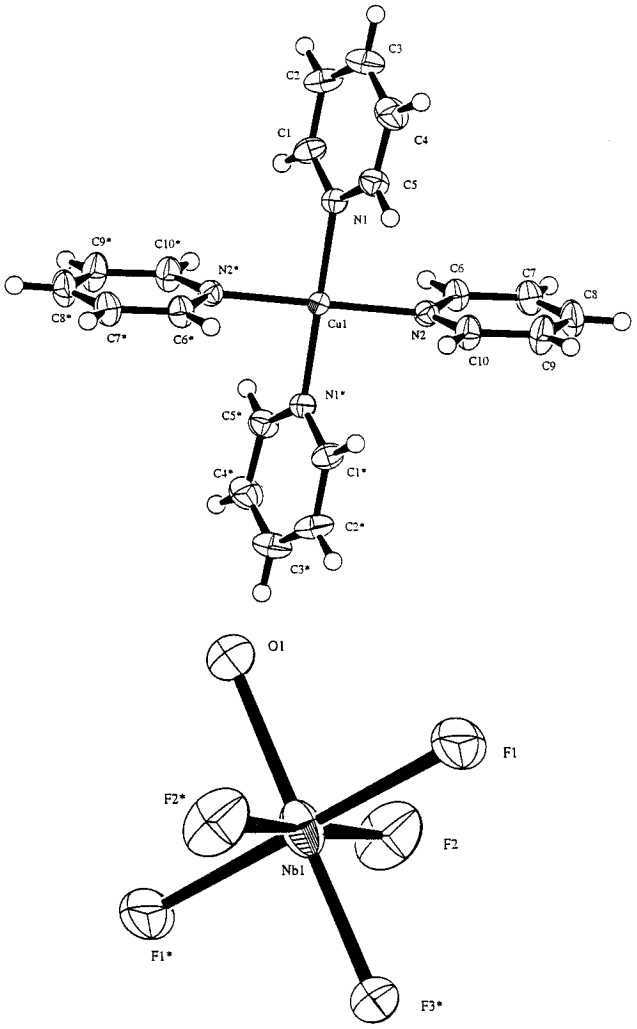

Figure 5. ORTEP (50% probability) plots of $[Cu(py)_4]^{2+}$ and $[NbOF_5]^{2-}$.

The use of bond valence[31] provides some insight into the coordination and structural differences of $[pyH^+]_2[CuNb_2(py)_4O_2F_{10}]^{2-}$ and $CuNb(py)_4OF_5$. For the $[CuNb_2(py)_4O_2F_{10}]^{2-}$ anion, the cationic charge on Cu^{2+} is largely distributed on the pyridine rings, +0.4 for each group, owing to the strong Cu−N bonds. The weak Cu−O bonds result in very strong Nb−O bonds, with a valence of 1.64, which predictably leads to the distorted Nb^V environment. Within the Nb^V octahedra, each Nb−F bond has a valence of 0.7, resulting in each fluorine having an anionic charge of −0.3. It is interesting to speculate that the crystallization fields of $[pyH^+]_2[CuNb_2(py)_4O_2F_{10}]^{2-}$ and $CuNb(py)_4OF_5$ are controlled by the concentration of pyridinium poly(hydrogen fluoride). In the former, the anionic $[CuNb_2(py)_4O_2F_{10}]^{2-}$ clusters are linked through N−H···F interactions with the $[pyH^+]$ cations, while in $CuNb(py)_4OF_5$ the two $[pyH^+]$ cations have been replaced by $[Cu(py)_4]^{2+}$.

The structure of $CuNb(py)_4OF_5$ may be described either as noncentrosymmetric (space group *Cc*, No. 9) with ordering of the bridging oxygen and fluorine or as centrosymmetric (space group *C*2/*c*, No. 15) with disorder in these atoms. A strong intraoctahedral distortion of this $[NbOF_5]^{2-}$ group should be observed in space group *Cc*. The centrosymmetric−noncentrosymmetric (disorder−order) dilemma has been discussed by Marsh,[32] who argues in favor of describing structures in the centrosymmetric space group with disorder (unless a clear choice

(30) Gill, N. S.; Nuttall, R. H.; Scaife, D. E.; Sharp, D. W. A. *J. Inorg. Nucl. Chem.* **1961**, *18*, 79.

(31) Brown, I. D.; Altermatt, D. *Acta Crystallogr.* **1985**, *B41*, 244.

(32) Marsh, R. E. *Acta Crystallogr.* **1986**, *B42*, 193.

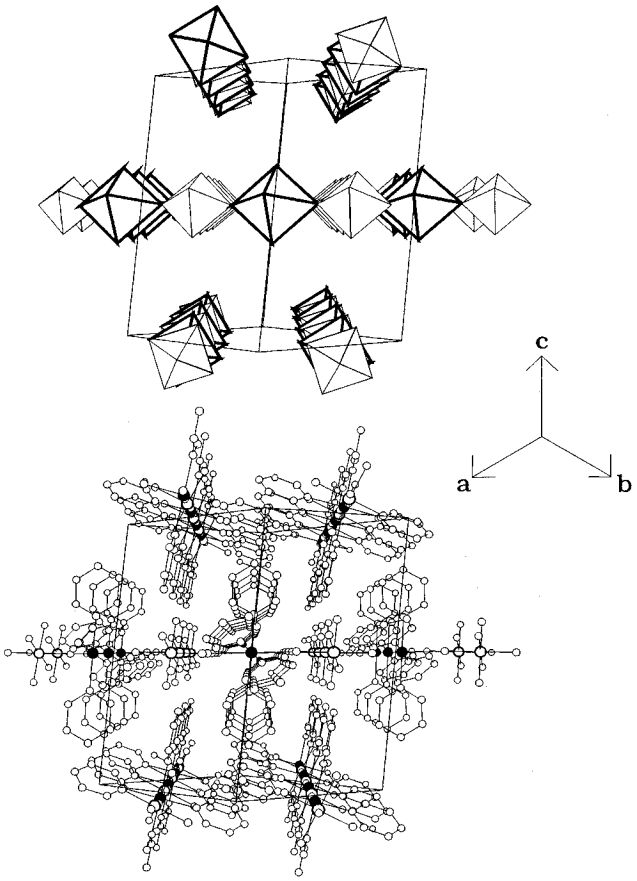

Figure 6. Polyhedral and ball-and-stick representations of $CuNb(py)_4OF_5$. The copper octahedra are dark, and the niobium octahedra are light. In the ball-and-stick diagram, the Cu^{II} atoms are black circles and the Nb^V atoms are dark outlined circles. F(1) and F(2) are both singly bonded, and F(3) and O(1) are disordered over the bridging site. Note the 90° rotation of the corner-shared, one-dimensional octahedral chains every *c*/2.

can be made in favor of the noncentrosymmetric space group), because of ill-behaved refinements in the noncentrosymmetric space group. The perils of *Cc* have been elucidated;[33] in fact, of all 230 space groups, *Cc* is the most frequently assigned incorrectly. The centrosymmetric disordered model of $CuNb(py)_4OF_5$ is consistent with the null result from the powder SHG measurements, concordant with a cancellation of the expected intraoctahedral distortion of the $[NbOF_5]^{2-}$ group. This cancellation can occur by an *interchain* or *intrachain* mechanism. However, owing to poor local charge balance of the intrachain model, some form of interchain disorder is probable. A compound of the same stoichiometry, prepared at room temperature by simply mixing separate solutions of $CuCO_3$ and Nb_2O_5 dissolved in aqueous HF (40%) and pyridine, has been reported.[34] Characterization of this powder was limited to elemental analysis and infrared spectroscopy.

Conclusion

In the search for new mixed-metal oxyfluorides with the FOJT Cu^{II} and the SOJT Nb^V, $[pyH^+]_2[CuNb_2(py)_4O_2F_{10}]^{2-}$ and $CuNb(py)_4OF_5$ were discovered in the course of studying the (CuO, $^1/_2Nb_2O_5$)/(HF)$_x$·pyridine/H_2O composition space. The pyridinium poly(hydrogen fluoride) concentration appears to be a controlling factor in whether $[pyH^+]_2[CuNb_2(py)_4O_2F_{10}]^{2-}$ or $CuNb(py)_4OF_5$ is formed. Decreasing the pyridine:metal ratio can be expected to strongly affect crystallization fields. The inclusion of polarizable octahedra such as $[NbOF_5]^{2-}$ is a necessary but not sufficient first step in the synthesis of potentially new optical materials. Rational chemical syntheses that control crystallization in piezoelectric or polar (ferroelectric) crystal classes present challenging problems deserving more study.

Acknowledgment. The authors gratefully acknowledge support from the National Science Foundation, Solid State Chemistry (Award No. DMR-9412971), and made use of the MRL Central Facilities supported by the National Science Foundation, at the Materials Research Center of Northwestern University (Award No. DMR-9120521). We also wish to acknowledge Rachel Bain for her assistance with the infrared spectra. Finally, we wish to acknowledge helpful suggestions from one of the reviewers on the subject of bond valence.

Supporting Information Available: Magnetic susceptibility plots and tables and an ORTEP (50% probability) plot of $[pyH^+]_2[CuNb_2(py)_4O_2F_{10}]^{2-}$ (5 pages). Two X-ray crystallographic files, in CIF format, are available. Access and/or ordering information is given on any current masthead page.

IC951189W

(33) Baur, W. H.; Kassner, D. *Acta Crystallogr.* **1992**, *B48*, 356.
(34) Sengupta, A. K.; Mandal, N. G. *Indian J. Chem.* **1976**, *15A*, 357.